British Journal of Applied Science & Technology
6(3): 239-260, 2015, Article no.BJAST.2015.084
ISSN: 2231-0843

SCIENCEDOMAIN *international*
www.sciencedomain.org

Experimental Investigations on DI Diesel Engine with Different Combustion Chambers Insulation

M. V. S. Murali Krishna[1*], N. Janardhan[2], CH. Kesava Reddy[1] and P. V. K. Murthy[3]

[1]Department of Mechanical Engineering, Chaitanya Bharathi Institute of Technology, Gandipet, Hyderabad 500075, Telangana State, India.
[2]Mahatma Gandhi Institute of Technology, Gandipet, Hyderabad- 500075, Telangana State, India.
[3]Jaya Prakash Narayan Educational Society Group of Institutions, Mahabubnagar 509001, Telangana State, India.

Authors' contributions

This work was carried out in collaboration between all authors. Authors MVSMK and PVKM designed the study, performed the statistical analysis, wrote the protocol, and wrote the first draft of the manuscript. Authors CHKR and NJ managed the literature searches. All authors read and approved the final manuscript.

Article Information

DOI: 10.9734/BJAST/2015/13865
Editor(s):
(1) Elena Lanchares Sancho, Department of Mechanical Engineering, University of Zaragoza, Spain.
(2) Manoj Gupta, Department of Mechanical Engineering, National University of Singapore, Singapore.
(3) Harry E. Ruda, Centre for Advanced Nanotechnology, University of Toronto, Canada.
Reviewers:
(1) Anonymous, India.
(2) Hasan Aydoğan, Selcuk University, Turkey.
(3) Sajjad Soleimani, Laboratory of Biological Structure Mechanics, Department of Chemistry, Materials, and Chemical Engineering "Giulio Natta," Politecnico di Milano, Milan, Italy.
(4) Anonymous, India.
Complete Peer review History: http://www.sciencedomain.org/review-history.php?iid=766&id=5&aid=7343

Original Research Article

Received 6th September 2014
Accepted 15th November 2014
Published 16th December 2014

ABSTRACT

Aim: The four-stroke single cylinder diesel engine's performance with various low heat rejection (LHR) combustion chambers was determined Critical comparison was made for various configurations of the combustion chambers with neat diesel operation.
Design Parameters: Direct injection diesel engine with various configurations of the combustion chambers–Combustion chamber with air gap insulation and ceramic coating (LHR–3); air gap insulation (LHR–2); and ceramic coated combustion chamber (LHR–1) Injection pressure and timing.

**Corresponding author: E-mail: Krishnamurthy_venkata@yahoo.co.in, maddalivs@gmail.com, narambhatlu.datta@gmail.com;*

Materials and Methods: Exhaust emissions and performance parameters and were evaluated at different values of brake mean effective pressure (BMEP) of the engine. Combustion parameters were evaluated at its peak load operation. Particulate emissions were determined by smoke opacity meter (AVL 437), while nitrogen oxide levels were noted by NOx Analyzer (Netel Chromatograph NOx Analyzer (VM 4000). Combustion characteristics of the engine were determined at peak load operation of the engine using TDC (top dead centre) encoder, miniature Piezo electric pressure transducer, and special p (pressure)–θ (crank angle) software package.
Brief Results: Deteriorated performance was shown by the engine with air gap insulated and ceramic coated (LHR–3) combustion chamber, when compared with engine with other configurations of the combustion chamber at recommended injection timing of 27° bTDC.(before top dead centre)
Conclusions: Engine with LHR–1, LHR–2 and LHR–3 combustion chambers with mineral diesel operation showed deteriorated performance at 27° bTDC and improved at optimum injection timings and with increased injection pressure.

Keywords: Performance; Emissions; Combustion parameters; Injection Pressure; Injection timing.

1. INTRODUCTION

Due to their durability and high fuel efficiency, diesel engines have become popular power plants for the applications of automotive industry. This is globally the most accepted type of internal combustion engine used for powering industrial applications, agricultural implements, marine propulsions, along with construction equipment. In view of heavy consumption of diesel involved in not only agricultural sector and but also in transport sector and also its depletion, the energy conservation has become essential, which has been the concern of the researchers, users, and manufacturers involved in combustion & alternate fuel research.

II law of Thermodynamics finds the inevitable heat loss to the coolant to consider the output. Any saving in this part of the energy share would either increase power output or increase the energy lost through exhaust gases. Various researchers adopted different methods to decrease heat loss to the coolant. Three approaches that are being tried to decrease heat loss to the coolant are ceramic coating and air gap insulation (1), air gap insulation (2) and ceramic coating (3).

Ekerm et al. [1] carried out experiments on direct-injection, six–cylinder, turbocharged diesel engine with pistons coated with a 0.350 mm thickness of $MgZrO_3$ over a 0.150 mm thickness of NiCrAl bond coat. $CaZrO_3$ as the coating material for valves and cylinder head. It was reported from their experiments that reduction of BSFC of 1–8% with the combined effect of the injection timing and thermal barrier coating (TBC). Nitrogen oxide emissions were decreased by 11% at 18° bTDC compared with base engine. Engine with ceramic coated combustion chamber reduced BSFC by 6% when compared with base engine with neat diesel operation [2]. Ciniviz et al. [3] reported that diesel engine with ceramic coated cylinder head increased torque by 2% and decreased BSFC at full load operation by 4.5–9% when compared base engine.

Joining two different metals in creating an air gap in the piston involved the complications. Welding design adopted by Parker in making air gap in the piston could not provide complete sealing of air [4]. The two part piston of engine with LHR combustion chamber consisted of crown with a low thermal conductivity material, superni (an alloy of nickel) threaded to aluminum body of the piston, providing a 3 mm air gap in between these two parts by providing gasket with thickness of 3 mm with engine was operated with advanced injection timing [5]. There was reduction of BSFC at part loads by 12% and 4% at full load at 29.5° bTDC with the engine with two part insulated piston when compared with standard engine at 27° bTDC [5]. Murali Krishna carried out investigations with engine with an air gap insulated piston with crown made of superni and an air gap insulated liner provided with superni insert with diesel fuel. It was reported from his investigations that engine with LHR combustion chamber reduced pollution levels and improved its performance at 80% of the peak load operation and performance was deteriorated beyond this load [6].

Krishna Murthy conducted experiments on engine with LHR-3 combustion chamber with neat diesel and reported that insulated engine showed deterioration n its performance at all

loads at 27° bTDC. However, It improved at 28° bTDC [7].

Efficient combustion in diesel engine resulted with an increase injection pressure [8-11]. Formation of pollution levels and performance will be effected with increased injection pressure. Different researchers used various configurations of the engine with insulated combustion chambers. Experimental studies were conducted on engine a cast iron piston with an air gap and Nimonic alloy crown in which the bottom surface was coated with 0.5 mm thick layer of stabilized zirconia (LHR–1 combustion chamber), .an air gap piston with a Nimonic alloy crown (LHR–2 combustion chamber), cast iron piston with an air gap of 4mm and Nimonic alloy crown (LHR–3 combustion chamber) and cast iron piston (LHR–4 combustion chamber); [12]. BTE was increased by 3%, volumetric efficiency was decreased by 13% and there was a drastic reduction of smoke levels with engine with LHR-1 combustion chamber when compared with base engine.

Performance was evaluated with four–stroke, 3.68 kW Kirloskar diesel engine at a speed of 1500 rpm and compression ratio of 16:1 at recommended injection timing of 27° bTDC and with varied injector opening pressure with different combustion chambers–LHR–1, LHR–2 and LHR–3 with mineral diesel operation [13-16]. Performance improved with increased degree of insulation. However, experiments were conducted at 27° b TDC.

Here, there was an attempt to make comparative studies with engine with various combustion chambers such as conventional combustion chamber, LHR–1, (ceramic coated cylinder head); LHR–2 (air gap insulted piston and air gap insulated liner); and LHR–3 (ceramic coated cylinder head, air gap insulated piston and air gap insulated liner) with varied injection pressure and timing.

2. MATERIALS AND METHODS

Table 1 shows the properties of neat diesel.

2.1 Engine with LHR Combustion Chamber

Engine with LHR–3 combustion chamber consisted of a two–part piston (Fig. 1) the top crown with superni was threaded to body of the piston, providing 3 mm air gap in between these two parts, by providing a superni gasket in between body and crown of the piston. A superni insert was threaded to the top portion of the liner so as to keep an air gap of 3 mm between the insert and the body of the liner.

Coating of partially stabilized zirconium (PSZ) of thickness 500 microns was provided on inside portion of cylinder head by means of plasma coating technique. Table 2 presents the properties of superni and partially stabilized zirconium. The application of these low thermal conductivity materials of superni, air and PSZ provided resistance to the heat flow to the coolant, which resulted engine with LHR–3 combustion chamber. Engine with LHR–2 combustion chamber consisted of air gap insulated piston and air gap insulated liner. Engine with LHR–1 combustion chamber contained only ceramic coating on inside portion of cylinder head. From LHR–1 to LHR–3 combustion chamber, there was increase of degree of Insulation.

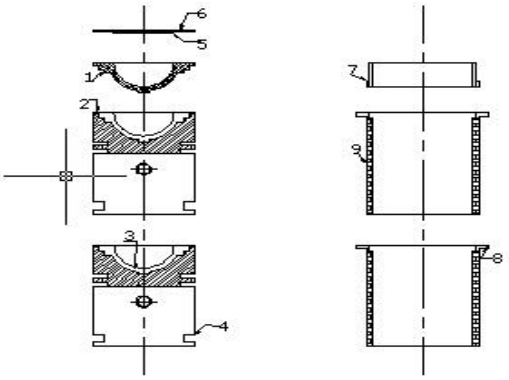

Fig. 1. Assembly details of air gap insulated piston, air gap insulated liner and ceramic coated cylinder head

1.Piston crown with threads, 2.Superni gasket, 3. Air gap in piston, 4. Body of piston. 5. Ceramic coating on inside portion of cylinder head, 6. Cylinder head, 7.Superni insert for liner, 8.Air gap in liner and 9. Liner

2.2 Experimental Set–Up

2.2.1. Performance parameters

Fig. 2 shows the schematic diagram of the experimental setup used for the studies on the engine with various combustion chambers with mineral diesel. Table 3 shows the specification of the experimental engine (Component No. 1). For measuring brake power of the engine, it was connected to an electric dynamometer (Component No. 2). Kirloskar make. Loading rheostat (Component No. 3) loaded the dynamometer. The accuracy of engine load was

found to be ±0.2 kW by uncertainity analysis. Engine speed was determined with digital tachometer with accuracy ±1%. Engine air consumption was obtained with an assembly of an orifice meter (Component No. 4)), U–tube water manometer (Component No. 5) and air box (Component No. 6). For finding fuel consumption of the engine, Burette (Component No.9) method was employed with the help of fuel tank ((Component No. 7) and three way valve (Component No. 8). The accuracy of brake thermal efficiency determined by uncertainity analysis was found to be ±2%.

The diaphragm of an air–box was used to damp out the engine's pulsations for ensuring a steady flow of air through the engine intake manifold. The engine was water cooled engine in which outlet temperature of water of 80°C was maintained by adjusting the water flow rate, determined by water flow meter (Component No. 14) and its flow rate was measured by means of analogue water flow meter, with accuracy of measurement of ±1%. There was pressure feed system for engine oil. There was no temperature control for measuring the temperature of the lube oil. Injection pressure was varied from 190 bar to 270 bar by nozzle testing device. The maximum injector opening pressure was confined to 270 bar due to existence of practical difficulties.

Table 1. Properties of diesel fuel

Property	Units	Diesel (DF)	ASTM standard
Carbon chain	--	C_8-C_{28}	
Density	gm/cc	0.84	ASTM D 4809
Kinematic viscosity at 40°C	cSt	3.18	ASTM D 445
Lower calorific value	MJ/kg	44.8	ASTM D 240
Cetane Number	---	55	ASTM D 613
Oxygen	%	0.3	---
Flash Point	°C	68	ASTM D93
Fire Point	°C	103	---
Pour Point	°C	-7	---
Air fuel ratio (Stochiometric)	--	14.86	---
Bulk modulus @ 20 Mpa	Mpa	1475	---
Sulfur	%	0.25	ASTM D93
Colour	--	Light yellow	---

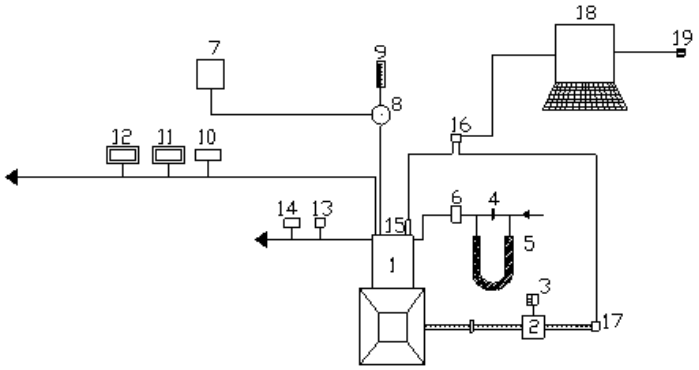

Fig. 2. Schematic diagram of experimental Set-up

1.Engine, 2.Electical Dynamometer, 3.Load Box, 4.Orifice meter, 5.U–ube water manometer, 6.Air box, 7.Fuel tank, 8, Three–way valve, 9.Burette, 10. Exhaust gas temperature indicator, 11.Smoke opacity meter, 12. NOx Analyzer, 13.Outlet jacket water temperature indicator, 14. Outlet-jacket water flow meter, 15.Piezo-electric pressure transducer, 16.Console, 17.TDC encoder, 18.Pentium Personal Computer and 19. Printer

Change of injection timing was achieved by incorporating copper shims between pump body and engine frame. Exhaust gas temperature (EGT) and coolant water outlet temperatures were measured with iron-constantan thermocouples provided to the exhaust gas temperature indicator (Component No. 10) and outlet jacket temperature indicator (Component No 13). The accuracies of analogue temperature indicators obtained by uncertainity analysis are ±1%.

2.2.2 Exhaust Emissions

The exhaust emissions from diesel engine are particulate emissions and nitrogen oxide levels. When they are inhaled, they create health hazards, like headache, lung cancer, tuberculosis, respiratory problems, dizziness, nausea, hemorrhage and skin cancer [17]. They polluted containing CO_2 released from automobiles reach ocean in the form of acid rain, there by polluting water. Hence control of these emissions is an important and urgent task.

Exhaust emissions of particulate matter and NO_x were measured by Smoke opacity meter (AVL India, 437) (Component No. 11) and NO_x analyzer (Netel Chromatograph, 4000 VM) (Component No. 12) at various values of BMEP of the engine. Table 4 shows the measurement principle, range, least count, and repeatability of analyzers for recording particulate emissions and nitrogen oxide levels.

2.2.3. Combustion Characteristics

Water-cooled piezoelectric pressure transducer (AVL, Austria: QC34D). (Part No. 15) determined in-cylinder pressure, while crank angle up to resolution of 0.5 was obtained with a precision shaft encoder (AVL, Austria: 365x) (Part No. 17). Cylinder head was provided with Piezo electric transducer, to determine pressure in the combustion chamber and this transducer was connected to a console (Part No. 16) which was connected to personal computer (Part No. 18) and printer (Part No. 19). TDC encoder, used to determine the crank angle the engine was employed at the extended shaft of the dynamometer was connected to the console. A pressure-crank angle software determined the combustion characteristics such as peak pressure (PP), time of occurrence of peak pressure (TOPP) and maximum rate of pressure rise (MRPR) from the signals of crank angle and pressure at the full load operation of the engine. Pressure-crank angle diagram was obtained on the screen of the personal computer. The accuracy of measurement of is found to be ±1° for crank angle, while it is ±1 bar for pressure.

2.3 Test Conditions

Mineral diesel was used as test fuel. Different combustion chambers used for the engine were conventional combustion chamber, LHR–1, LHR–2 and LHR–3. Various injection pressure tried in this experiment were 190 bar and 270 bar. Each test was conducted twelve times to ensure the reproducibility of data according to uncertainity analysis (Minimum number of trials must be more than ten).

2.4 Uncertainty Analysis

Uncertainty analysis gives top priority to make a technical contribution to decision-making through the quantification of uncertainties, involved in the relevant variables.

Inphysical experiments, experimental uncertainty or assessment uncertainty analysis provides with assessing the uncertainty or error in a measurement. An experiment demonstrate a law, or estimate the numerical value of a physical variable or designed to determine an effect, will be affected by errors due to instrumentation, presence of confounding effects methodology, and so on. Experimental uncertainty estimates are required to estimate the confidence in the results [18].

Reality is much more complex as a calibrated parameter does not necessarily represent reality. Any prediction or estimation has its own complexities of reality that cannot be represented uniquely in the measured value, leading to make a probable error. Such error must be taken into consideration, in order to provide management decisions on the basis of model outcomes [19]. Reality was not represented with a calibrated parameter, as it is more complex. Any prediction or estimation has its own complexities of reality that cannot be represented uniquely or precisely in the calibrated model; therefore, potential error is bound to happen. When making management decisions on the basis of model outcomes, such error must be accounted. The accuracy of a measurement system is the degree of closeness of measurements of a quantity to that quantity's actual (true) value in the fields of engineering, industry, statistics and science. The precision of a measurement system, related

to repeatability and reproducibility is the degree to which repeatability of measurements under without changing conditions show the same results [18,19]. Although the two words accuracy and precision can be synonymous in colloquial use, they are widely contrasted in the view of the scientific method. A measurement system can be precise but not accurate, accurate but not precise, neither, or both. Appendix-1 shows the detailed discussion on results of uncertainity analysis.

3. RESULTS AND DISCUSSION

Fig. 3 indicates that brake thermal efficiency (BTE) increased with increase of BMEP up to 4.2 bar with mineral diesel and beyond that load, it decreased at injection timing of 27° bTDC. Increase of mechanical efficiency, volumetric efficiency and fuel conversion efficiency were the reasons for increase of BTE up to 80% of the full load, while reduction of volumetric efficiency, air–fuel ratios and fuel conversion efficiency were responsible factors to decrease BTE beyond 80% of the full load. With advanced injection timing, CE with diesel operation increased BTE at all loads. This was due to increase of resident time of fuel and initiation of combustion at early period with air leading to improve atomization. At an optimum injection timing of 31° bTDC, CE with diesel operation increased peak BTE by 11% in comparison with 27° bTDC.

Fig.4 shows that that engine with LHR–1 combustion chamber at 27° bTDC showed comparable performance when compared with CE 27° bTDC with neat diesel operation. This was due to evaporation rate of fuel in hot environment provided by hot combustion chamber of LHR engine and improved heat release and At optimum injection timing of 30° bTDC, engine with LHR-1 combustion chamber with neat diesel increased its peak BTE by 4% when compared with CE at 27° bTDC.

Fig. 5 shows that that engine with LHR–2 combustion chamber at 27° bTDC with neat diesel increased BTE with increase of BMPE up to 80% of peak load operation at 27° bTDC, and beyond that it reduced, in comparison with CE at 27° bTDC. This was due to higher degree of insulation provided in the piston and liner, with the provision of an gap with superni inserts, decreased the heat rejection causing to improve BTE. However peak BTE with engine with LHR–2 combustion chamber decreased beyond 80% of full load, in comparison with CE. This was because of reduction of ignition delay. At an optimum injection timing of 29° bTDC, this drawback disappeared which showed that a significant part of the exhausted or rejected heat was directly converted to useful work at piston, rather than being merely wasted through the exhaust stream.

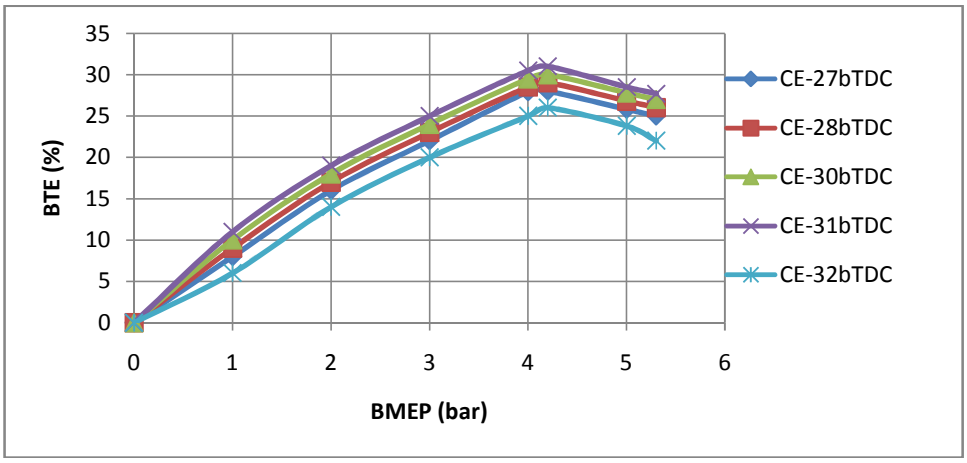

Fig. 3. Variation of brake thermal efficiency (BTE) with brake mean effective pressure (BMEP) with conventional engine

Table 2. Properties of PSZ and Superni material

Material	Allowable temperature (o C)	Strength (MPa)	Density (gm/cc)	Thermal conductivity (W/m-K)	Specific Heat (J/kg-K)	Thermal expansion coefficient (10^{-6}/K)	Young's Modulas (Gpa)
PSZ	1000	200–1000	5.2–6.1	2.2-3.8	400-700	8.0–11.4	140–210
Superni	1400	700–1100	8.0	12	461	13	200

Table 3. Specifications of the test engine

Description	Specification
Engine make and model	Kirloskar (India) AV1
Maximum power output at a speed of 1500 rpm	3.68 kW
Number of cylinders ×cylinder position× stroke	One × Vertical position × four-stroke
Bore × stroke	80 mm × 110 mm
Engine Displacement	553 cc
Method of cooling	Water cooled
Rated speed (constant)	1500 rpm
Fuel injection system	In-line and direct injection
Compression ratio	16:1
BMEP @ 1500 rpm at full load	5.31 bar
Manufacturer's recommended injection timing and injector opening pressure	27° bTDC × 190 bar
Number of holes of injector and size	Three × 0.25 mm
Type of combustion chamber	Direct injection type
Fuel Injection Nozzle	Make: MICO-BOSCH: No- 0431–202–120/HB
Fuel Injection pump	Make: BOSCH: NO– 8085587/1

Table 4. Specifications of the Smoke Opacimeter (AVL, India, 437) and exhaust gas emission analyzer (Netel Chromatograph NO_x Analyzer (4000 VM))

Pollutant	Measuring principle	Range	Least count	Repeatability
Smoke opacity	Light extinction	1–100%	0.2% of full scale (FS)	0.1% for 30 minutes
NO_x	Chemiluminiscence	1–5,000 ppm	0.5% FS	≤0.5%FS

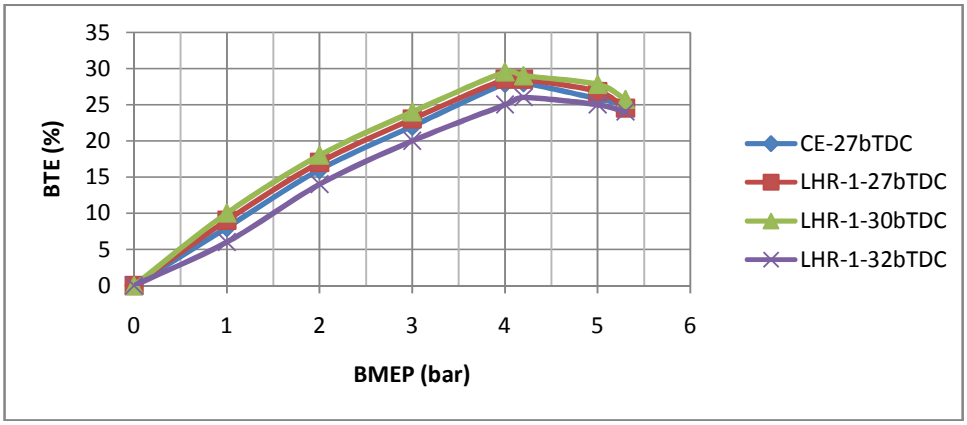

Fig. 4. Variation of brake thermal efficiency (BTE) with engine with LHR–1 combustion chamber

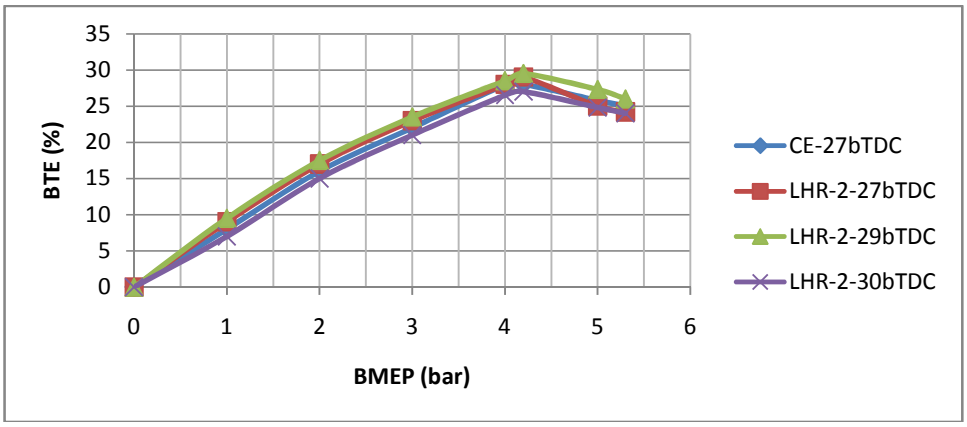

Fig. 5. Variation of brake thermal efficiency (BTE) with engine with LHR–2 combustion chamber

When compared with CE, at 27° bTDC engine with LHR–2 combustion chamber increased peak BTE by 3% at 29° bTDC. Engine with LHR-2 combustion chamber with mineral diesel operation showed improved performance (coolant load, volumetric efficiency and exhaust gas temperature) up to 80% of the peak load at 27° bTDC and beyond that load, deteriorated of performance was observed, when compared with CE. This was because of improved combustion with improved fuel conversion efficiency up to 80% of the peak load operation and deteriorated its performance at near peak load because of decrease of ignition delay. Earlier researcher on this aspect made similar observations [6].

Fig.6, indicates that engine with LHR–3 combustion chamber with mineral diesel showed deteriorated performance at all loads, when compared with CE at an injection timing of in 27° bTDC. This was because of reduction of ignition delay, which reduced pre–mixed combustion as a result of which, less time was available for proper mixing of diesel and air and diesel fuel leading to incomplete combustion. More over at full load, increased diffusion combustion and friction resulted from reduced ignition delay. Increased radiation losses were one of the reasons for the deterioration. However, due to atomization of fuel, performance improved with advanced injection timing. Peak BTE was increased by 6% at its optimum injection timing of 28° bTDC, in comparison with CE at 27° bTDC. Earlier researcher on this aspects made similar observations [7].

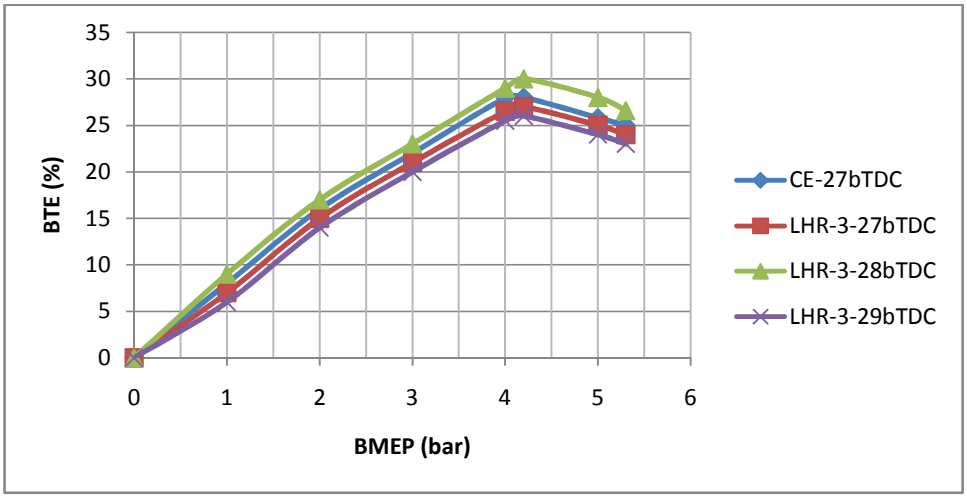

Fig. 6. Variation of brake thermal efficiency (BTE with engine with LHR–3 combustion chamber

The optimum injection timings with engine with different combustion chambers were shown in Table 5. The optimum injection timings was observed to be 31° bTDC with CE, while they were 30° bTDC, 29° bTDC and 28° bTDC engine with LHR-1, LHR–2 and LHR–3 combustion chambers with diesel operation.

From combustion chambers, LHR-1 to LHR-3, there was increase of degree of insulation. The optimum injection timing was found to be reduced with an increase of degree of insulation. Hot combustion chamber of LHR engine decreased ignition delay and combustion duration. Hence with an increase of degree of insulation, the optimum injection timing was obtained earlier.

Fig. 7 indicates that engine with LHR–3 combustion chamber at 27° bTDC, with neat diesel operation showed reduced peak BTE, in comparison with other configurations of the combustion chamber. This was because of decrease of ignition delay. With advanced injection timing, peak BTE increased with different configurations of the combustion chamber. This was due to increase of resident time of fuel with air, thus improving combustion. CE at 31° bTDC, showed increase of peak BTE in comparison with other versions of the combustion chamber, as its optimum injection timing was observed to be higher, when compared with other configurations of the insulated combustion chamber.

At recommended injection timing, engine with LHR–1, LHR–2 and LHR–3 combustion chamber with mineral diesel showed higher peak BTE by 2%, 3% and reduced by 3% in comparison with CE. At optimum injection timings, they decreased peak BTE by 6%, 5% and 3% when compared with CE at its optimum injection timing.

Table 5. Optimum injection timing with diesel operation recommended injection timing-27° Btdc

Combustion chamber	Optimum injection timing (Degree before TDC)
CE	31
LHR–1	30
LHR–2	29
LHR–3	28

Fig. 8, which represents the variation of brake specific fuel consumption (BSFC) followed similar trends as shown in Fig. 7. At recommended injection timing, engine with LHR–3 combustion chamber showed higher BSFC at full load operation, while CE at its optimum injection timing showed lower BSFC. This was due to because of decrease of ignition delay with the engine with LHR–3 combustion chamber. At the recommended injection timing, engine with LHR–1, LHR–2 and LHR–3 combustion chamber with mineral diesel increased BSFC at peak load by 2%, 3% and 4%, when compared with CE. At optimum injection timings, while increasing it by 8%, 7% and 4% in comparison with CE at its optimum injection timing. Decrease of fuel–air ratio and volumetric efficiency were responsible factors for higher BSFC with engine with different configurations of the LHR combustion chambers, in comparison with CE.

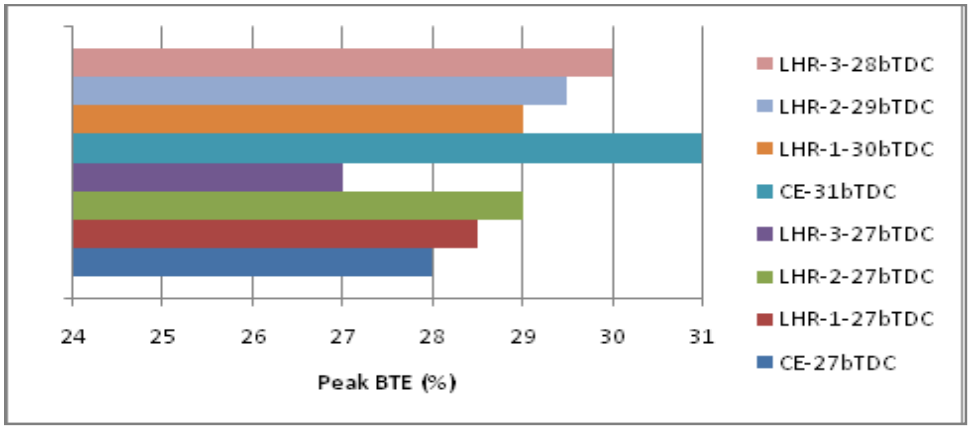

Fig. 7. Variation of peak brake thermal efficiency

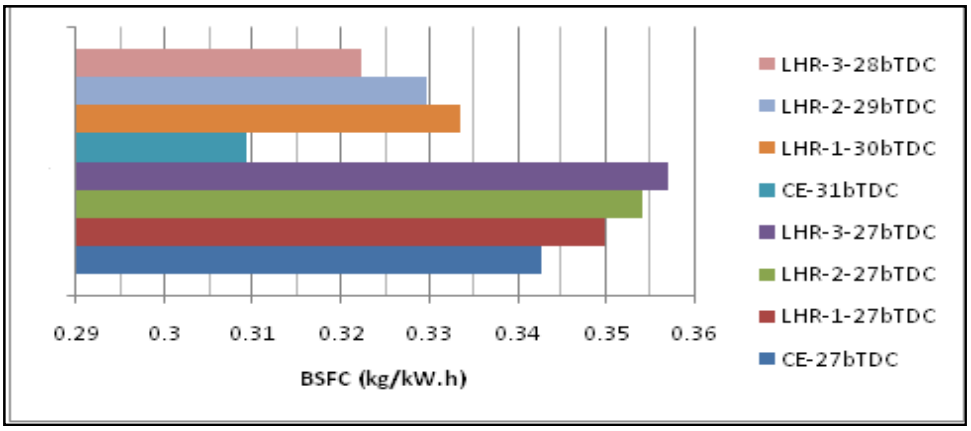

Fig. 8. Variation of brake specific fuel consumption (BSFC) at full load operation

From Fig. 9, it is noticed that exhaust gas temperature (EGT) at full load operation with mineral diesel decreased with increase of advanced injection timing. This was due to the conversion of heat into useful work with advanced injection timing. EGT at full load increased with increase of degree of insulation with mineral diesel. This shows that heat rejection was confined in combustion chamber, which maintains combustion chamber hot, with which EGT at full load increased with increase of degree of insulation.

At recommended injection timing, engine with LHR–1, LHR–2 and LHR–3 combustion chamber with diesel operation showed higher EGT at peak load by 3%, 12% and 18%, in comparison with CE. They showed higher EGT at peak load by 12%, 20% and 27% in co at optimum injection timing, when compared with CE its optimum injection timing.

From Table 6, it is noticed that peak BTE, BSFC at full load and EGT at full load with engine with different configurations of the combustion chamber were marginally improved with increased injection pressure.

With an increase of injection pressure, droplet diameter decreased, which influences the quality of the atomization, and hence more dispersion of fuel particle, causing enhanced mixing o fuel with air, leads to improved fuel-oxygen mixing rate, as it was reported extensively in the literature [8–11]. Fig. 10 indicates that CE increased coolant load at peak load, while engine with different LHR combustion chambers reduced coolant load with advanced injection timing. In case of CE, because of effective utilization of energy liberated from combustion, un–burnt fuel concentration decreased, causing increase of coolant load with mineral diesel fuel at peak load operation. However, the improvement in the performance of the CE with diesel was due to

rejection at lower temperatures and heat addition at higher temperatures. In case of engine with LHR combustion chambers, it was due to reduction of gas temperatures with improved fuel-oxygen ratios. Reduction of coolant load at peak load was observed with an increase of degree of insulation. At recommended injection timing, engine with LHR–1, LHR–2 and LHR–3 combustion chamber with mineral diesel reduced coolant load by 3%, increased it by 5% and reduced it by 5% when compared with CE. In case of engine with LHR-2 combustion chamber, this was due to increase of gas temperatures and rejection of heat through un-insulated portion of combustion chamber. Other researcher made similar observations [6]. At optimum injection timings, engine with different configurations of LHR combustion chambers decreased coolant load at peak load by 9%, 12% and 15% in comparison with CE at its optimum injection timing. This was due to reduction of gas temperatures with provision of thermal insulation with engine with different versions of the LHR combustion chambers.

From Fig. 11, it is observed that engine with different versions of the combustion chamber increased volumetric efficiency at full load operation marginally with advanced injection timing. This was because of reduction of combustion wall temperatures which in turn depends on EGT. At 27° bTDC, engine with LHR–1, LHR–2 and LHR–3 combustion chamber with mineral diesel reduced volumetric efficiency at full load by 6%, 7% and 8% when compared with CE, while at optimum injection timings, they decreased it by 9%, 10% and 11% in comparison with CE at 31° bTDC. This was because of increase of temperature of incoming charge in the hot environment with the provision of insulation, making decrease in the density and hence the quantity of air.

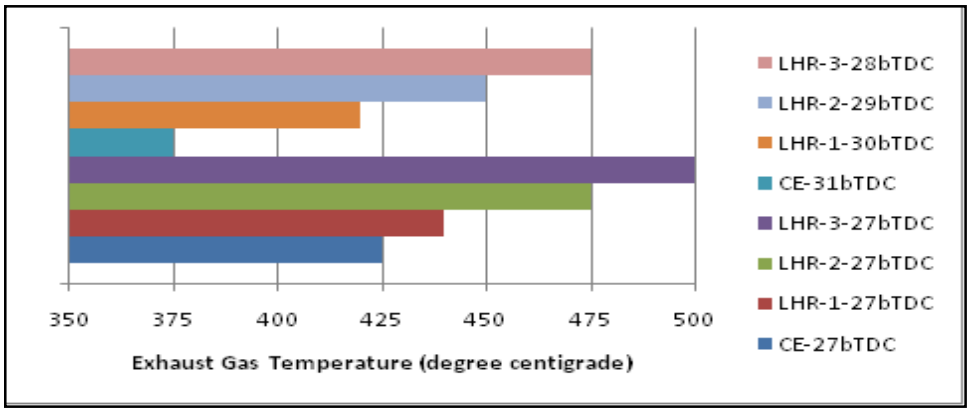

Fig. 9. Variation of exhaust gas temperature at full load operation

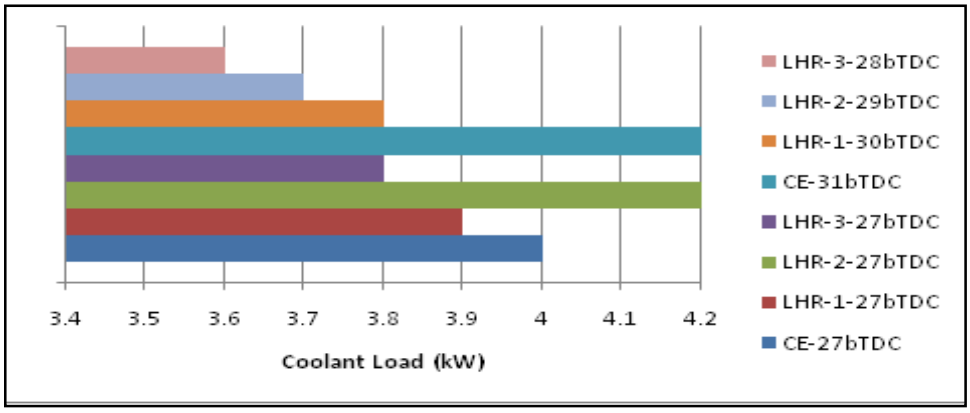

Fig. 10. Variation of coolant load at full load operation

Table 6. Data of peak brake thermal efficiency, BSFC and EGT at full load operation

Injection timing (°bTDC)	Engine version	Peak BTE (%)		BSFC (kg/k W.h)		Exhaust gas temperature (°C)	
		Injector opening pressure (bar)		Injector opening pressure (bar)		Injector opening pressure (bar)	
		190	270	190	270	190	270
	CE	28	30	0.3428	0.3188	425	395
27	LHR–1	28.5	29.5	0.3498	0.3375	440	400
	LHR–2	29	30	0.3541	0.3418	475	425
	LHR–3	27	29	0.3570	0.3305	500	450
30	LHR–1	29	30	0.3335	0.3220	420	380
29	LHR–2	29.5	30.5	0.3296	0.3280	450	400
28	LHR–3	30	31.5	0.3223	0.3008	475	425
31	CE	31	30	0.3094	0.3193	375	425

Table 7 indicated that increase of coolant load with CE, while decreasing it with different versions of the LHR combustion chamber with an increase of an injection pressure.

This was because increased injection pressure increased nominal fuel spray velocity, resulting in improved fuel–air mixing with which gas temperatures increased in CE.

Decrease of coolant load in engine with different configurations of the insulated engine was due to improved fuel spray characteristics and increase of oxygen–fuel ratios causing reduction of gas temperatures and hence the coolant load. Earlier researchers made similar studies and confirmed the trends as observed by the authors [13–16].

Table 7 indicates that increase of volumetric efficiency with engine with different versions of the combustion chamber with increased injection pressure. This was because of improved spray characteristics of the fuel and reduction of EGT at full load operation. Similar trends were observed by earlier studies [13–16].

3.2 Exhaust Emissions

In compression ignition engines, it is rather difficult to reduce particulate emissions and nitrogen oxide levels simultaneously due to soot–NO_x tradeoff. High particulate emissions and nitrogen oxide levels are still the main obstacle in the development of next generation conventional diesel engines. Fig. 12, indicates that particulate emissions increased with increase of BMEP with engine with different configurations of the combustion chamber. The particulate emissions were more or less constant up to 80% of the full load operation, due to presence of excess amount of oxygen. Beyond that load, particulate emissions increased drastically due to lack of available oxygen in these fuel–rich zones, causing incomplete combustion. This was also because of cracking of fuel cracking at higher temperature, leading to increase in particulate matter density. The drastic increase of particulate emissions at near full load operation was because of decrease of volumetric efficiency, air-fuel ratio and fuel conversion efficiency. Engine with LHR–2 combustion chamber showed improved particulate emissions up to 80% of the full load operation due to increase of volumetric efficiency, air–fuel ratios and volumetric efficiency beyond that load, it increased the same over and above CE because of decrease of ignition delay. Earlier researcher made similar observations on the aspect of particulate emissions [6].

Fig. 13 indicates that particulate emissions at full load operation reduced with advanced injection timing with engine with different versions of the combustion chamber. This was because of increase of oxygen–fuel ratios, causing effective combustion in different configurations of LHR combustion chambers at their optimum injection timings. This was due to increase of fuel atomization. However fuel droplet size also increased due to lower cylinder temperatures and pressures prevailing at the time of advanced fuel injection. These two factors affected the formation of particulate formation in opposite direction. However, particulate emissions reduced with advanced injection timing with the combined effect of these two factors. Other researchers made similar observations [8–11].

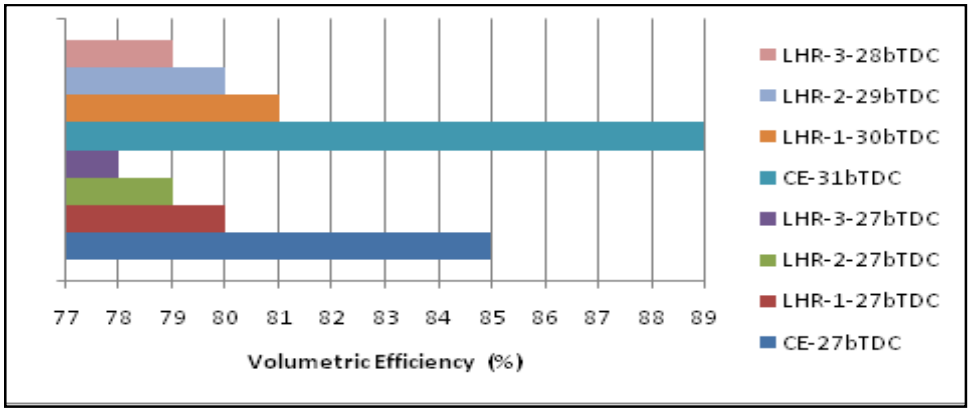

Fig. 11. Variation of volumetric efficiency at full load operation

Table 7. Data of coolant load and volumetric efficiency at full load operation

Injection timing (°bTDC)	Engine version	Coolant load (kW)		Volumetric efficiency (%)	
		Injector opening pressure (bar)		Injector opening pressure (bar)	
		190	270	190	270
	CE	4.0	4.4	85	87
	LHR–1	3.9	3.5	80	82
27	LHR–2	4.2	3.8	79	81
	LHR–3	3.8	3.4	78	80
30	LHR–1	3.8	3.4	81	83
29	LHR–2	3.7	3.2	80	82
28	LHR–3	3.6	3.0	79	81
31	CE	4.2	4.6	89	87

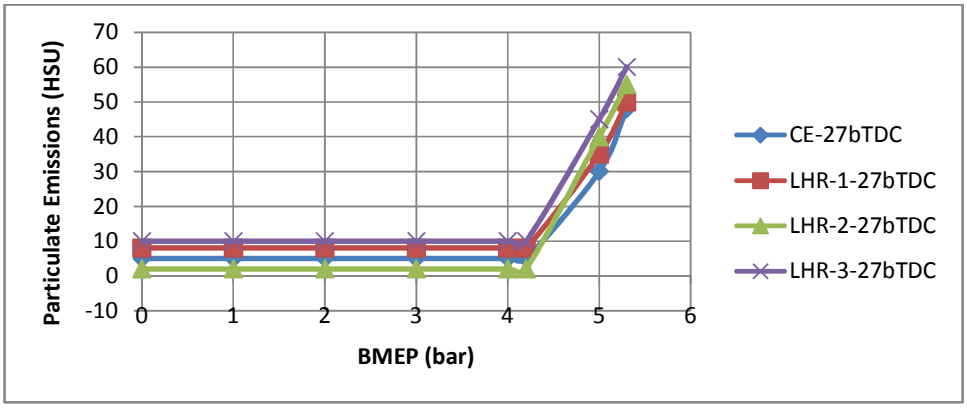

Fig. 12. Variation of particulate emissions in Hartridge Smoke Unit (HSU) with brake mean effective pressure (BMEP)

Increase of degree of insulation increased particulate emissions. This was because of fuel cracking at higher temperatures existing in insulated combustion chamber. At recommended injection timing, engine with LHR–1, LHR–2 and LHR–3 combustion chamber with mineral diesel increased particulate emissions at full load by 4%, 15% and 25% in comparison with CE. At optimum injection timing, increased particulate emissions at full load by 14%, 33% and 50% in comparison with CE.

Fig. 14 indicates that nitrogen oxide levels (NO_x) levels increased with an increase of BMEP with

mineral diesel with engine with different configurations of the combustion chamber at 27° bTDC. This was because of increase of combustion temperatures with increased fuel consumption. NO_x levels at full load operation were observed to be higher as air-fuel ratios were approaching to theoretical air fuel ratio. Engine with LHR–2 combustion chamber showed decrease of NO_x levels up to 80% of the full load operation due to availability of excess air with improved volumetric efficiency and oxygen–fuel ratios, and beyond that load, it increased the same over and above CE, because of enriched air fuel ratio which are approaching to stoichiometric value. Earlier researcher made similar observations on the aspect of nitrogen oxide levels. Earlier researcher made similar observations on this aspect [6].

At 27° bTDC, engine with different versions of LHR combustion chambers with mineral diesel showed higher NO_x levels at full load operation than CE. This was because of increase of combustion temperatures with the improved combustion and heat release rates in the engine Earlier researchers made similar observations on this aspect [6,13-16].

Fig. 15 indicates that NO_x levels at full load operation increased with CE, while engine with different LHR combustion chambers showed decrease of the same with advanced injection timing. Increase of resident time and combustion temperatures for NO_x chemistry to take place leading to generate higher NO_x levels in the exhaust of CE, while decrease of gas temperatures with improved fuel–fuel ratios reduced NO_x levels in engine with engine with different versions of the LHR chamber.

At recommended injection timing, engine with LHR–1, LHR–2 and LHR–3 combustion chamber with mineral diesel increased NO_x levels at full load by 41%, 47% and 53% in comparison with CE.

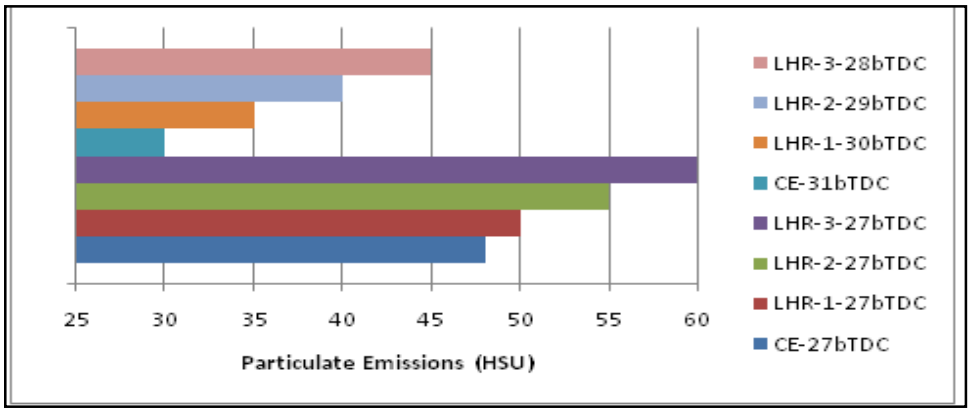

Fig. 13. Variation of particulate emissions at full load operation

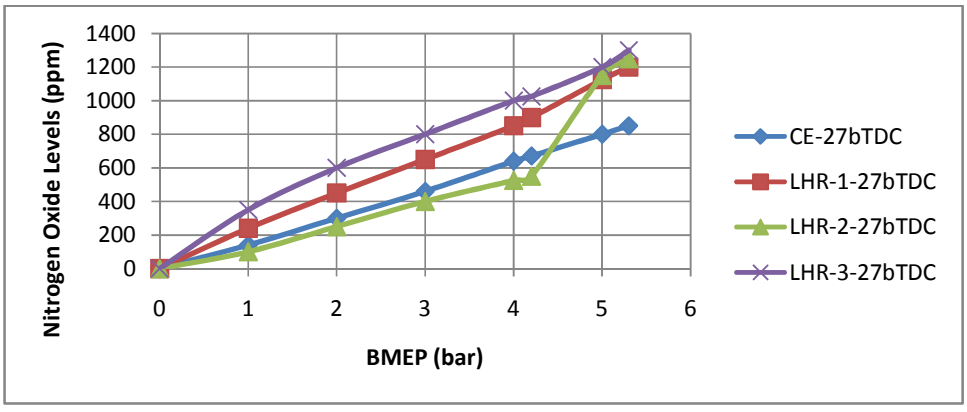

Fig. 14. Variation of nitrogen oxide (NOx) levels with brake mean effective pressure (BMEP)

At optimum injection timings, they decreased NOx levels at full load operation by 5%, showed comparable value and increased by 5%, in comparison when compared with CE. This was because of reduction of gas temperatures at advanced injection timing with different configurations of the LHR combustion chamber.

Table 8 denotes that particulate emissions at full load operation on engine with different configurations of the combustion chambers reduced with increased injection pressure. This was because of improved fuel spray characteristics at higher injection pressure leading to decrease particulate emissions. Higher fuel injection pressures improved air–fuel mixing followed by faster combustion which directly influences pollutant formation causing reduction of particulate emissions. At higher injection pressures, total particulate number concentration in the exhaust of the engine reduced due to relatively superior fuel–air mixing. Depth of penetration of fuel in air zone increased with increased injection pressure causing improved atomization leading to reduce particulate emissions at peak load operation with engine with different configurations of the combustion chamber. Earlier researchers made similar observations on this aspect with CE [8–11].

From same table, it is observed that CE increased NO_x levels, while engine with different configurations of the LHR combustion chambers reduced the same with increased injection pressure. This was because of enhanced spray characteristics, thus improving air fuel mixture preparation and evaporation process in CE, with which gas temperatures increased causing increase of nitrogen oxide levels in CE. Earlier researchers made similar observations on this aspect with CE [8–11]. Improved combustion with improved oxygen–fuel ratios in engine with different versions of the LHR combustion chamber causing reduction of gas temperatures and hence NO_x levels. Earlier researchers made similar observations on this aspect with engine with LHR combustion chamber [13–16].

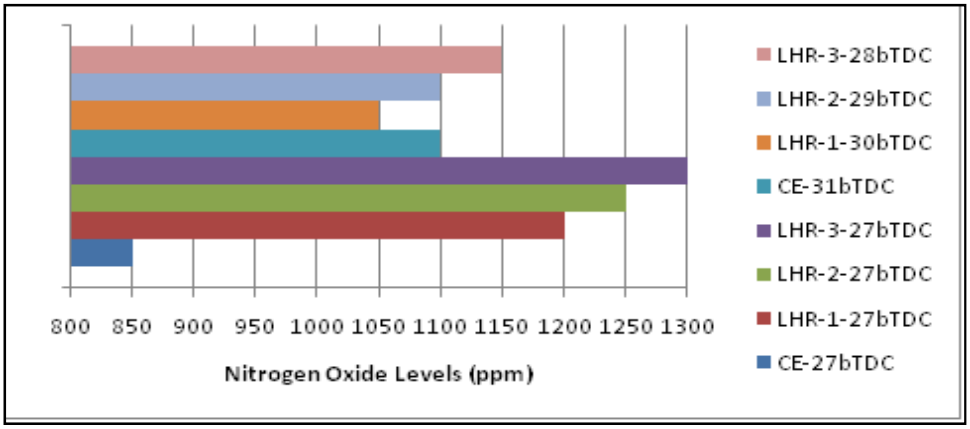

Fig. 15. Variation of nitrogen oxide levels at full load operation

Table 8. Data of particular emissions and nitrogen oxide levels at full load operation

Injection timing (°bTDC)	Engine version	Particulate emissions (HSU)		Nitrogen oxide levels (ppm)	
		Injector opening pressure (bar)		Injector opening pressure (bar)	
		190	270	190	270
	CE	48	34	850	950
27	LHR–1	50	40	1200	1100
	LHR–2	55	45	1250	1150
	LHR–3	60	50	1300	1200
30	LHR–1	35	25	1050	950
29	LHR–2	40	30	1100	1000
28	LHR–3	45	35	1150	1050
31	CE	30	40	1100	1200

Higher fuel-injection pressures will reduce the rich zone fuel-air ratio prevailing in the core of the spray, which leads to lower soot formation. This may increase the surface area of the 'stochiometric diffusion flame sheet, which in turn increases NO_x formation and emission with CE. Earlier researchers made similar observations on this aspect with CE [8–11].

3.3 Combustion Characteristics

Fig. 16 shows that CE with mineral diesel increased peak pressures at peak load operation, while engine with different configurations of the LHR combustion chamber marginally reduced the same with advanced injection timing. This was because of increased ignition delay of fuel in CE, causing sudden increase of peak pressures with the accumulated fuel with advanced injection timings. Improved combustion with improved fuel-air ratios reduced peak pressure at full load operation on engine with different configurations of the insulated combustion chamber with advanced injection timing. PP drastically increased with increased degree of insulation. This was because of increase of gas temperatures with decrease of ignition delay. At recommended injection timing, engine with LHR–1, LHR–2 and LHR–3 combustion chamber with mineral diesel increased PP at full load by 9%, 20% and 32% in comparison with CE. At optimum injection timings, they decreased PP by 13%, 7% and increased the same by 2%, in comparison with CE. This was because of increase of gas temperatures with faster evaporation of fuel injected into hot combustion chamber of different versions of LHR engine at recommended injection timing. Reduction of gas temperatures with improved fuel– oxygen ratios were responsible factors for reduction of PP in engine with various configurations of the combustion chamber. Earlier researchers made similar observations with engine with insulated combustion chamber [13–16].

Fig. 17 followed similar trends as PP at full load operation with engine with various configurations of combustion chamber. At optimum injection timing, engine with LHR–1, LHR–2 and LHR–3 combustion chamber with mineral diesel increased maximum rate of pressure rise (MRPR) at peak load by 26%, 33% and 41% in comparison with CE. At optimum injection timings, engine with LHR–1 combustion chamber showed comparable value, while engine with LHR–2 and LHR–3 combustion chambers increased it by 13% and 16%, in comparison with CE. This was because of highly volatile nature of mineral diesel causing instantaneous burning in hot environment, which was provided by engine with insulated combustion chamber. Earlier researchers made similar observations with engine with insulated combustion chamber [13-16].

Table 9 denotes that PP and MRPR at peak load operation increased with CE, while marginally reducing it with engine with various insulated combustion chamber with increased injection pressure with neat diesel. This may be due to smaller sauter mean diameter shorter breakup length, improved dispersion and atomization characteristics. This improves combustion rate in the premixed combustion phase in CE. Earlier researchers made similar observations with CE [8–11]. Improved combustion with improved air–fuel ratios marginally decreased PP and MRPR at peak load operation with engine with insulated combustion chamber. Earlier researchers made similar observations with engine with insulated combustion chamber [13–16].

Table 9 denotes that time of occurrence of peak pressure (TOPP) at peak load operation reduced (towards TDC) with engine with different configurations of the combustion chamber with the advanced injection timing, which confirmed that combustion improved with advanced injection timing. TOPP at peak load full load operation was higher at recommended injection timing with engine with different versions of the combustion chamber when compared with CE. This was due to the engine with insulated combustion chamber exhibited higher temperatures of combustion chamber walls causing continuation of combustion, giving PP away from TDC. However, at their optimum injection timing, this phenomenon was nullified due to reduced temperature of combustion chamber walls thus bringing the peak pressures nearer to TDC. TOPP at peak load operation reduced marginally with increased injection pressure with test fuels as observed from same table. This was because of improved spray characteristics and reduction fuel particle size. Earlier researchers made similar observations with engine with insulated combustion chamber. [13–16].

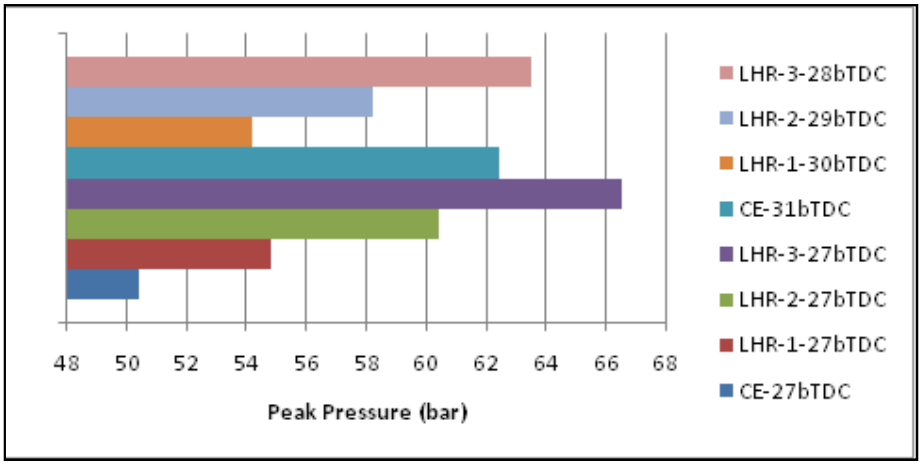

Fig. 16. Variation of peak pressure at full load operation

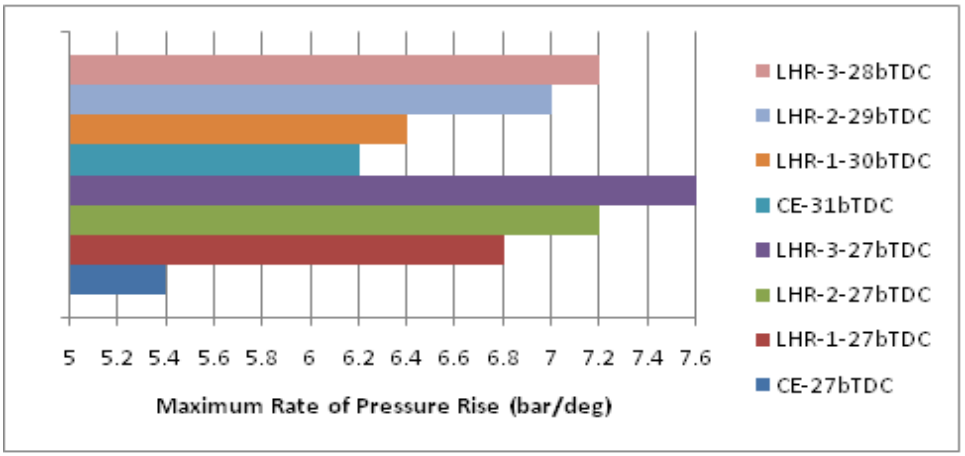

Fig. 17. Variation of maximum rate of pressure rise at full load operation

Table 9. Data of combustion characteristics at full load operation

Injection timing (°bTDC)	Engine version	Peak pressure (bar)		MRPR (bar/degree)		TOPP (Degrees before TDC)	
		Injector opening pressure (bar)		Injector opening pressure (bar)		Injector opening pressure (bar)	
		190	270	190	270	190	270
	CE	50.4	53.5	5.4	6.0	9	9
27	LHR–1	54.8	50.8	6.8	6.2	10	8
	LHR–2	60.4	56.7	7.2	6.4	10	8
	LHR–3	66.5	60.6	7.6	6.8	10	9
30	LHR–1	54.2	50.2	6.4	6.0	9	7
29	LHR–2	58.2	54.4	7.0	6.2	9	7
28	LHR–3	63.5	59.5	7.2	6.4	9	8
31	CE	62.4	60.6	6.2	5.6	8	9

4. CONCLUSION

1. The optimum injection timing was observed to be 31° bTDC with conventional engine (CE), while they were 28° bTDC, 29° bTDC and 30° bTDC for engine with LHR–1, LHR–2 and LHR–3 combustion chamber at an injector opening pressure of 190 bar with diesel operation. Hot combustion chamber of LHR engine reduced ignition delay and combustion duration and hence the optimum injection timing was obtained earlier with increased degree of insulation.
2. At recommended injection timing, the engine with different configurations of insulated combustion chamber showed deteriorated performance at peak load operation, when compared with CE with diesel operation. This was due to decrease of ignition delay
3. At optimum injection timings, the engine with various configurations of the insulated combustion chamber showed comparable performance with CE at recommended injection timing of 27° bTDC with diesel operation. At optimum injection timings, engine with LHR–1, LHR–2 and LHR–3 combustion chambers with mineral diesel decreased BSFC at full load by 3%, 4% and 6% in comparison with CE at 27^{o} bTDC. This was because of improved atomization with advanced injection timing.
4. At optimum injection timings, engine with LHR–1, LHR–2 and LHR–3 combustion chambers with mineral diesel decreased particulate emissions at full load by 27%, 17% and 6% when compared with CE at 27^{o} bTDC. This was due to increase of contact of fuel with air leading to reduce particulate emissions.
5. At optimum injection timings, engine with LHR–1, LHR–2 and LHR–3 combustion chambers with mineral diesel increased nitrogen oxide levels at full load by 23%, 29% and 35% when compared with CE at 27° bTDC. This was due to increase of gas temperatures with improved heat release rate.
6. Performance parameters, pollution levels and combustion characteristics improved with increased injection pressure and advanced injection timing with engine with various versions of combustion chamber with diesel. This was due to improved spray characteristics, depth of penetration of fuel in air zone, and atomization of the fuel.

5. RESEARCH FINDINGS

Comparative studies were made on performance parameters, pollution levels and combustion characteristics for engine with different configurations of the insulated combustion chamber and CE with mineral diesel with varied injection pressure and injection timing.

6. HIGHLIGHTS

- Fuel injection pressure & injection timings affect engine performance, exhaust emissions and combustion characteristics.
- Emission characteristics improve with advanced fuel injection timings with engine with different configurations of the insulated combustion chambers.
- Engine performance, exhaust emissions and combustion characteristics were influenced by degree of insulation provided with LHR combustion chamber.

7. NOVELTY

Injection timing was varied by inserting copper shims in between pump body and engine frame. The performance of the engine along with pollution levels and combustion characteristic with different configurations of insulated combustion chamber with mineral diesel operation was investigated and comparative studies were made with CE working on similar working conditions.

8. SCIENTIFIC SIGNIFICANCE

Engine with LHR combustion chamber decreased particulate emissions, which cause impact on health and environment. In diesel engines, it is rather difficult to lower NO_x and particulate matter emissions simultaneously due to soot-NO_x tradeoff. High NO_x and particulate matter emissions are still the main obstacle in the development of next generation conventional diesel engines. However, the increased nitrogen oxide levels with engine with LHR combustion chamber can be controlled by suitable chemical treatment. Engine performance was improved with change of combustion chamber design and varied engine parameters like injection pressure and injection timing.

9. SOCIAL SIGNIFICANCE

Energy conservation is an important measure of fuel crisis. Increase of fuel prices in International Market which causes economic burden on developing countries in importing crude petroleum, which otherwise can be spent in important sectors like poverty, health , education, industry etc.

10. FUTURE SCOPE OF STUDIES

Engine with LHR combustion chamber increased NO_x emissions. However, NO_x levels in engine with insulated combustion chamber can be controlled by means of the selective catalytic reduction (SCR) technique using lanthanum ion exchanged zeolite (catalyst–A) and urea infused lanthanum ion exchanged zeolite (catalyst–B) with different versions of combustion chamber at full load operation of the engine [20]. The other method to reduce NO_x levels is by blending of ethanol or methanol in small quantities with diesel.

ACKNOWLEDGMENTS

Authors thank authorities of Chaitanya Bharathi Institute of Technology, Hyderabad for providing facilities for carrying out this research work. Financial assistance provided by All India Council for Technical Education (AICTE), New Delhi is greatly acknowledged.

COMPETING INTERESTS

Authors have declared that no competing interests exist.

REFERENCES

1. Ekrem B, Tahsin E, Muhammet C. Effects of thermal barrier coating on gas emissions and performance of a LHR engine with different injection timings and valve adjustments. Energy Conversion and Management. 2006;47:1298–1310.
2. Parlak A, Yasar H, ldogan O. The effect of thermal barrier coating on a turbocharged diesel engine performance and exergy potential of the exhaust gas. Energy Conversion and Management. 2005;46(3): 489-499.
3. Ciniviz M, Hasimoglu C, Sahin F, Salman MS. Impact of thermal barrier coating application on the performance and emissions of a turbocharged diesel engine. Proc. The Institution of Mechanical Engineers Part D-Journal of Automobile Eng. 2008;222(D12):2447-2455.
4. Parker DA, Dennison GM. The development of an air gap insulated piston. SAE Paper 870652; 1987.
5. Rama Mohan K, Vara Prasad CM, Murali Krishna MVS. Performance of a low heat rejection diesel engine with air gap insulated piston. ASME J Gas Turbines and Power. 1999;121 (3):530-540.
6. Murali Krishna MVS. Performance evaluation of low heat rejection diesel engine with alternate fuels. PhD Thesis, J. N. T. University, Hyderabad, Telangana State, India; 2004.
7. Krishna Murthy PV. Studies on biodiesel with low heat rejection diesel engine. PhD Thesis, J. N. T. University, Hyderabad, Telangana State, India; 2010.
8. Celikten I. An experimental investigation of the effect of the injection pressure on engine performance and exhaust emission in indirect injection diesel engines. Appl Therm Eng. 2003;23:2051–60.
9. Cingur Y, Altiparmak D. Effect of cetane number and injection pressure on a di diesel engine performance and emissions. Energy Conversion and Management. 2003;44:389–397.
10. Hountalas DT, Kouremenos DA, Binder KB, Schwarz V, Mavropoulos GC. Effect of injection pressure on the performance and exhaust emissions of a heavy duty di diesel engine. SAE Technical Paper No. 2003-01-0340. Warrendale, PA.
11. Avinash Kumar Agarwal, Dhananjay Kumar Srivastava, Atul Dhar, et al. Effect of fuel injection timing and pressure on combustion, emissions and performance characteristics of a single cylinder diesel engine. Fuel. 2013;111:374–83.
12. Jabez Dhinagar S, Nagalingam B, Gopala Krishnan KV. A comparative study of the performance of a low heat rejection engine with four different levels of insulation. Proc. of IV Int Conference on Small Engines and Fuels Chang Mai, Thailand. 1993;121-26.
13. Murali Krishna MVS, Janardhan N, Murthy PVK, Ushasri P, Nagasarada S. A comparative study of the performance of a low heat rejection diesel engine with three different levels of insulation with vegetable

oil operation. Archive of Mech Eng. 2012;1:101-128.

14. Kesava Reddy Ch, Murali Krishna MVS, Murthy PVK, Ratna Reddy T. A comparative study of the performance evaluation of a low heat rejection engine with three different levels of insulation with crude pongamia oil operation, Canadian Journal on Mechanical Sciences & Engineering. 2012;3(3):59–71.
15. Murali Krishna MVS, Chowdary RP, Kishan Kumar Reddy T, Murthy PVK. A comparative study of the performance of a low heat rejection diesel engine with three different levels of insulation with waste fried vegetable oil operation. International Journal of Science & Technology. 2012;2(6):358–371.
16. Ratna Reddy T, Murali Krishna MVS, Kesava Reddy Ch, Murthy PVK. Comparative performance of different versions of the low heat rejection diesel engine with mohr oil based bio-diesel. Int J Res & Reviews in Appl Sciences. 2012;1(1):73-87.
17. Khopkar SM. Environmental pollution analysis. New Age International (P) Ltd, Publishers New Delhi. 2011;180-190.
18. John Robert Taylor. An introduction to error analysis: The Study of Uncertainties in Physical Measurements. University Science Books. 1999;128–129.

    ISBN: 0-935702-75-X.
19. Etienne de Rocquigny, Nicolas Devictor, Stefano Tarantola. Uncertainty in Industrial practice: A guide to quantitative uncertainty management, Wiley & Sons Publishers; 2008.
20. Janardhan N, Ushasri P, Murali Krishna MVS, Murthy PVK. Performance of biodiesel in low heat rejection diesel engine with catalytic converter, Int J Eng & Advanced Tech. 2012;2(2):97–109.

Appendix-01 (Uncertainity Analysis)

Case–01: Uncertainity Associated with Instrumentation

The exhaust gas temperature was found out with thermocouples made of iron-constantan connected to analogue exhaust gas temperature indicator

i. Range = 0—600°C
ii. Resolution = 5°C

Uncertainity or Absolute Error=1% of Reading + 2 Resolutions (Manufacturer's Recommendation) [18–19]

Exhaust gas temperature at full load operation with conventional engine with pure diesel operation = 425°C

Uncertainity = $\frac{1}{100} \times 425 + 2 \times 5$ = 15°C

Uncertainity in Reading = (425 + 15) — (425– 15)
= (440 — 410)°C.

% of Relative Error or % of Uncertainity, which is measure of Accuracy= $\frac{15}{425} \times 100 = 3.5\%$

% of Precision= $= \frac{Max.value\,of\ temp. - Min.value\,of\ temp.}{Average value}$

= $\frac{440-410}{425} = 7\%$

Case–02: Uncertainty Associated with Process

Measurement of peak brake thermal efficiency (BTE) with pure diesel operation with conventional engine at an injector opening pressure

Minimum number of trials = 10 according to Error Analysis

Mode value or Maximum Number of Occurrence = 28%

$$\bar{x} = Mean value = \sum_{i=1}^{N} x_i = \frac{336}{12} = 28\%$$

Standard deviation, based on sample

$$S_x = \left[\frac{1}{n-1}\sum_{i=1}^{n}[x_i - \bar{x}]^2\right]^{\frac{1}{2}} = \sqrt{\left[\frac{1}{12-01}\right]\sum_{1}^{12}[6]}$$

= $= 0..74$

Accuracy = $\frac{S_x}{\bar{x}} = \frac{0..74}{28.} \times 100 = 2.63\%$

$$\overline{S}_x = \frac{S_x}{\sqrt{n}} = \frac{2.63}{\sqrt{12}} = \frac{2.63}{\sqrt{12}} = 0.71$$

Case–01: Uncertainty involved the Process (Mineral Diesel-CE)

Parameter	Accuracy
Mass of fuel	2.94%
Peak BTE	2.63%
Exhaust gas temperature with CE at full load operation	0.86%
Coolant load with CE at full load operation	3.8%
Volumetric efficiency with CE at full load operation	3.4%
Particulate matter with CE at full load operation	6.0%
Nitrogen Oxide levels with CE at full load operation	1.7%
Peak Pressure with CE at full load operation	1.5%
Maximum Rate of Pressure Rise at full load operation	3.9%

Case–02: Uncertainty involved with instrumentation (Mineral Diesel-CE)

Instrument	Purpose	Accuracy
EGT indicator	For measuring EGT	3.5%
Tachometer	For measuring speed of the engine	1.3%
Burette	For measuring flow rate of fuel to the engine	1.1%
Stop watch	For noting down time taken for 10 cc of fuel	2.9%
Hydrometer	For measuring density of fuel	2.8%
Dynamometer	For measuring brake power of the engine	2.94%
Water flow meter	For measuring water flow rate to the engine	3.0%
Particulate Anlyzer	For measuring particulate emissions	4.16%
NOx Analyzer	For measuring nitrogen oxide levels	1.7%

Peer-review history:
The peer review history for this paper can be accessed here:
http://www.sciencedomain.org/review-history.php?iid=766&id=5&aid=7343